Acta Mech 228, 4425–4434 (2017)
DOI 10.1007/s00707-017-1942-0

ORIGINAL PAPER

A. K. Belyaev · V. V. Eliseev · H. Irschik · E. A. Oborin

Contact of two equal rigid pulleys with a belt modelled as Cosserat nonlinear elastic rod

Received: 12 October 2016 / Revised: 6 July 2017 / Published online: 18 August 2017

Abstract The setting of a looped drive belt on two equal pulleys is considered. The belt is modelled as a Cosserat rod, and a geometrically nonlinear model with account for tension and transverse shear is applied. The pulleys are considered as rigid bodies, and the belt–pulley contact is assumed to be frictionless. The problem has two axes of symmetry; therefore, the boundary value problem for the system of ordinary differential equations is formulated and solved for a quarter of the belt. The considered part consists of two segments, which are the free segment without the loading and the contact segment with the full frictionless contact. The introduction of a dimensionless material coordinate at both segments leads to a ninth-order system of ordinary differential equations. The boundary value problem for this system is solved numerically by the shooting method and finite difference method. As a result, the belt shape including the rotation angle, forces, moments, and the contact pressure are determined. The contact pressure increases near the end point of the contact area; however, no concentrated contact force occurs.

Mathematics Subject Classification 74K10 · 74B20 · 74M15

1 Introduction

The first systematic study of a belt drive (and elastic creep in it) was reported by Reynolds in [30], where he used the string model. Until recently, one-dimensional models of elastic strings were widely used, cf. [16,31,35]. The exact solution for nonlinear steady-state equations of the extensible string is obtained in [31] by assuming zones of the perfect and sliding friction contact between the belt and the pulley. A spatial description of the contour motion of the belt is suggested in [16]. An idealized point friction model allows extending this result to the transient dynamics, see [35].

However, it turned out that the model of extensible string describes just a part of important effects in the belt mechanics. The friction forces applied on the belt from the pulley result in a distributed moment. The

A. K. Belyaev
Institute for Problems in Mechanical Engineering, Russian Academy of Sciences, Saint Petersburg, Russia

V. V. Eliseev
Department of Mechanical Engineering and Design, Peter the Great Saint-Petersburg Polytechnic University, Saint Petersburg, Russia

H. Irschik · E. A. Oborin (✉)
Institute of Technical Mechanics, Johannes Kepler University, Linz, Austria
E-mail: evgenii.oborin@jku.at
Tel.: +43 732 2468 6280
Fax: +43 732 2468 6282

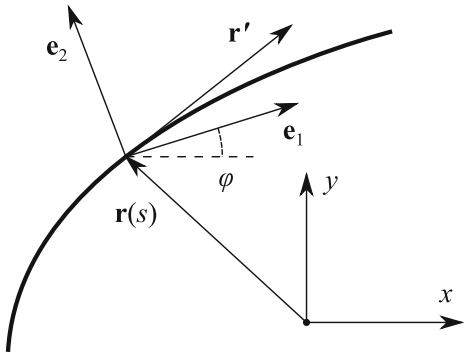

Fig. 1 Nonlinear elastic rod with account for shear and tension. Deformed configuration, unit vectors $\mathbf{e}_1$, $\mathbf{e}_2$, tangent vector $\mathbf{r}'$, reference Cartesian coordinate system and angle of deformed configuration φ

string model without bending stiffness cannot resist this loading. Therefore, we should use the rod model (i.e. the one with at least bending stiffness).

The calculation of the belt–pulley interaction can be found in [4,5,21,24,27,28,31]. It should be made with account for transverse shear. The importance of shear in contact problems of the rod theory is known, cf. [10,17,19,20]. The introduction of this deformation causes the absence of lumped contact forces and promotes better understanding of the contact force distribution. The shear is also required to describe the effect of elastic microslip, see, e.g. [8,25] for general friction modelling. Particularly, the shear is of importance in the operation of the friction belt drive [1,7,18,21].

However, the shear is known to be taken into account only together with the tension (compression) if the nonlinear theory of rods is applied. The goal of this work is to model the belt with bending and shear stiffness in the static contact problem of setting the belt on the pulleys. One finds the system of equations of the corresponding rod theory in [2,13,15,36] (without direct application to the belt-drive mechanics, though).

In the numerical modelling of the contact mechanics, the penalty formulation is in common use [37] and includes the choice of the penalty coefficient or its distribution (see e.g. [12] for the application in the contact between rods). This approach is applied for belt drives in [11,28,33].

In the present paper, we restrict ourselves to frictionless contact. We obtain the contact pressure and the stress–strain state in a different manner describing the form of the belt lying on the rigid pulley (the constraint formulation or the Hertz–Signorini–Moreau conditions for frictionless contact according to [37]). We assume that the contact is full in a classical sense, i.e. it is continuous in a single interval of the belt whose length is to be determined. In the present study, we use computer mathematics (the systems including both symbolic computation together with a user-friendly interface and numeric capabilities) to solve the difficult boundary value problems (BVP) for the systems of ordinary differential equations (ODE). The application of the standard numerical methods is possible due to the introduction of the transformed material coordinate. See [9,23] for an introduction into Mathcad and Mathematica, respectively; Wolfram Mathematica is efficiently used in the modern mechanics of thin-walled structures in [34].

In Sect. 2, we write down the equations of the nonlinear statics of rods. Then, we apply them to describe the belt equilibrium in the full contact segment where we assume that all points of this belt part lie on the pulley circle. In Sect. 3, we consider the free segment, i.e. the belt span. The absence of loads results in significant simplification of equations. The clear procedure of combining the equations for each segment into one system of ODE is also presented here. In Sect. 4, we discuss the variants of numerical solution of the formulated BVP. Finally, we show the results of numerical work and compare them with the previous results for the extensible model without shear [4] and the model without extension and shear [5]. A special case of different pulleys is studied in [6].

2 Equations of nonlinear contact problem

Figure 1 displays a general calculation scheme of the rod with shear and tension in the plane xy.

The rod is considered as a Cosserat line [2,13,15,36]. The position vector in the deformed configuration $\mathbf{r}(s)$ is a function of the material coordinate s and prime indicates differentiation with respect to s. The angular orientation of each particle of the rod is given by the orthonormal unit vectors $\mathbf{e}_1$, $\mathbf{e}_2$. The angle φ denotes the angle between the unit vector $\mathbf{e}_1$ and the Cartesian axis x, the latter having the unit vector $\mathbf{i}$.

For plane deformations, the system of equations of the nonlinear theory of rods is as follows [2,13,15,36]:

$$\begin{aligned}&\mathbf{Q}' + \mathbf{q} = 0, \quad M' + \mathbf{k}\cdot\mathbf{r}'\times\mathbf{Q} + m = 0,\\ &\varphi' - \varphi_0' = AM, \ \mathbf{r}' = \mathbf{P}\cdot\mathbf{r}_0{}' + \mathbf{B}\cdot\mathbf{Q} = \mathbf{e}_1(1 + B_1Q_1) + \mathbf{e}_2B_2Q_2.\end{aligned} \tag{1}$$

Here we denote: $\mathbf{Q}$ is the internal force vector, M is the bending moment, and $\mathbf{q}$, m stand for the external distributed forces and moments, respectively; $\mathbf{k}$ is the unit vector of the Cartesian axis z perpendicular to the drawing plane. The index zero indicates the values in the initial state, and $\mathbf{P} = \mathbf{e}_i\mathbf{e}_{i0}$ is the rotation tensor. Elastic characteristics of the rod in plane are determined by three scalar compliances: the bending compliance A, the tension compliance B_1, and the shear compliance B_2. The unit vectors $\mathbf{e}_1$, $\mathbf{e}_2$ are directed along the principal axes of the compliance tensor $\mathbf{B}$. The compliance tensors are determined by the three-dimensional theory of elasticity using two methods. First, we may utilize the solutions of the Saint-Venant problem comparing the complementary energies of the one- and three-dimensional solutions [14,15].[1] Second, we may provide the asymptotic analysis of the three-dimensional problem with the small thickness [15] (this approach is more difficult than the previous one). However, the calculation of the compliance tensors is a separate topic beyond the scope of this work, and we use the simple formulae for them in Sect. 4.

A way of solving BVP by means of computer mathematics for the system (1) is described in [23]. The algorithms and the results for the belt–pulley contact without shear are presented in [4,5]. The peculiarity of the considered problem is due to the fact that the function $\mathbf{r}(s) = \mathbf{R}(\sigma)$ is unknown in the contact segment because the arc coordinate σ is not yet determined.

We use the geometric relations and the expression of $\mathbf{r}'$ from (1):

$$\begin{aligned}&\mathbf{e}_1 = \mathbf{i}\cos\varphi + \mathbf{j}\sin\varphi, \ \mathbf{e}_2 = -\mathbf{i}\sin\varphi + \mathbf{j}\cos\varphi;\\ &\mathbf{r}'(s)\mathrm{d}s = \dot{\mathbf{R}}(\sigma)\mathrm{d}\sigma, \ \left|\dot{\mathbf{R}}\right| = 1,\\ &\sigma' = \left|\mathbf{r}'\right| \equiv D = \sqrt{(1 + B_1Q_1)^2 + (B_2Q_2)^2}, \ \dot{s} = D^{-1}.\end{aligned} \tag{2}$$

The equations in the third line determine the relation of the material coordinate s with the arc coordinate σ; a dot indicates the derivative with respect to σ.

Consider the full contact with the pulley. We write the expression for the tangent unit vector:

$$\dot{\mathbf{R}} = \mathbf{i}\sin\kappa\sigma + \mathbf{j}\cos\kappa\sigma, \ \mathbf{r}' = D\dot{\mathbf{R}} \tag{3}$$

and integrate it:

$$\mathbf{R} = \kappa^{-1}\left[\mathbf{i}\,(1 - \cos\kappa\sigma) + \mathbf{j}\sin\kappa\sigma\right]. \tag{4}$$

Here κ is the curvature of the pulley. Then, we assume $\mathbf{R}(0) = 0$ and note that

$$\begin{aligned}&\mathbf{r}'\cdot\mathbf{e}_1 = 1 + B_1Q_1 \ = D\sin(\varphi + \kappa\sigma),\\ &\mathbf{r}'\cdot\mathbf{e}_2 = B_2Q_2 = D\cos(\varphi + \kappa\sigma).\end{aligned} \tag{5}$$

Hence, it is possible to express the transverse force Q_2 as a function of the arc coordinate, angle, and the axial force in the following form:

$$\begin{aligned}&Q_2(\sigma, \varphi, Q_1) = B_2^{-1}(1 + B_1Q_1)\cot\alpha,\\ &\qquad \alpha(\sigma, \ \varphi) \equiv \varphi + \kappa\sigma.\end{aligned} \tag{6}$$

As a result, we have four unknown functions of s which are σ, φ, M, Q_1.

We assume no tangential contact between the belt and the pulley. Therefore, the vectors $\mathbf{q}$, $\mathbf{r}'$ are orthogonal:

$$\mathbf{Q}'\cdot\mathbf{r}' = 0; \quad \mathbf{e}_1{}' = \varphi'\mathbf{e}_2, \quad \mathbf{e}_2{}' = -\varphi'\mathbf{e}_1. \tag{7}$$

It yields:

$$(Q_1{}' - \varphi'Q_2)(1 + B_1Q_1) + (Q_2{}' + \varphi'Q_1)B_2Q_2 = 0. \tag{8}$$

[1] See the translation of paper [14] here: https://www.researchgate.net/publication/305990842.

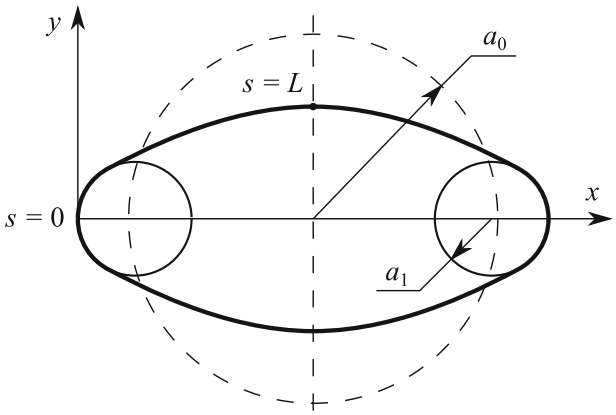

Fig. 2 Contact of belt and pulleys. The *thick line* is the deformed belt, the *dashed circle* is the undeformed belt, and the *thin circles* are the pulleys

In the last equation, we express the derivatives using (1), (2), and $Q_2 = Q_2(\sigma, \varphi, Q_1)$ as follows:

$$\begin{aligned} \varphi' &= \varphi_0{}' + AM, \\ Q_2{}' &= \frac{\partial Q_2}{\partial Q_1} Q_1{}' + \frac{\partial Q_2}{\partial \sigma} D + \frac{\partial Q_2}{\partial \varphi} \varphi' = \frac{B_1}{B_2} Q_1{}' \cot\alpha - \frac{1 + B_1 Q_1}{B_2 \sin^2\alpha} (\varphi' + \kappa\sigma'). \end{aligned} \tag{9}$$

The combination of (8) and (9) provides the differential equation for Q_1, which is not stated here for the sake of brevity. Then, we substitute $\mathbf{r}'$ from (1) into the balance of moment equation and obtain

$$M' = ((B_2 - B_1) Q_1 - 1)\, Q_2. \tag{10}$$

The expressions σ', φ', M', Q_1' form a fourth-order ODE system:

$$Y' = F(s, Y), \quad Y \equiv \begin{pmatrix} \sigma & \varphi & M & Q_1 \end{pmatrix}^{\mathrm{T}}. \tag{11}$$

Finally, we determine the contact pressure p:

$$Dp = \mathbf{q} \cdot \mathbf{k} \times \mathbf{r}' = \mathbf{k} \cdot \mathbf{Q}' \times \mathbf{r}' = (Q_1{}' - \varphi' Q_2) B_2 Q_2 - (Q_2{}' + \varphi' Q_1)(1 + B_1 Q_1). \tag{12}$$

The contact pressure must be nonnegative. Unlike the case without shear, in the considered problem there must be no concentrated contact reactions. The similar case of the classical contact between an initially straight nonlinear shearable rod and a rigid straight obstacle is discussed e.g. in [17].[2] The distributed contact moment which plays the key role in the elastic microslip (see [7]) in loaded drive vanishes because of the frictionless contact.

3 Contact of belt with pulleys

The scheme of setting the belt on the pulleys is shown in Fig. 2. In the initial state, the belt is the circle of radius a_0 (*dashed circle*). Hence, the initial angle and its derivative are $\varphi_0 = \pi/2 - a_0^{-1} s$, $\varphi_0' = -a_0^{-1}$. The pulleys are equal, and their radii are a_1. The centre distance (i.e. the distance between the pulley centres) is $2(a_0 - a_1) + \delta$, where the pulley displacement δ increases from zero under the force P that takes the pulleys apart.

Another point of view on a similar problem setting with the discussion of the physical nonlinearity and friction can be found in [26]. The belt tensioning is also studied in the encyclopaedic book [21] for an inextensible and unshearable belt model with bending stiffness and the straight initial configuration. An extension to quasi-static problem is investigated in [22].

[2] See the translation of paper [17] here: https://www.researchgate.net/publication/306058324.

Because of the problem symmetry, it is sufficient to consider only a quarter $0 \le s \le L = \pi a_0/2$. In the segment $0 \le s \le s_1$, the full contact is assumed; however, the coordinate s_1 is unknown. The formulation for this segment is presented above in Sect. 2.

Let us turn to the free segment $s_1 < s < L$. As follows from the force balance equation in (1), the force $\mathbf{Q}$ is constant. Using the symmetry, we can determine this force:

$$\mathbf{Q} = \frac{P}{2}\mathbf{i}. \tag{13}$$

The value P is prescribed; however, the dependence $\delta(P)$ should be determined. Due to the obvious absence of concentrated contact reaction at the point s_1, we have the continuity of $\mathbf{Q}$ (it also holds everywhere in the free segment):

$$Q_1 = \frac{P}{2}\cos\varphi, \quad Q_2 = -\frac{P}{2}\sin\varphi. \tag{14}$$

Since the force is constant, the equation of moments (1) is integrated:

$$M = \frac{P}{2}y + M_*. \tag{15}$$

The integration constant M_* can be determined using the continuity of the moment at the point s_1.

Then, we derive the following equations from (1):

$$\begin{aligned} \varphi' = -a_0^{-1} + AM,\ x' = (1 + B_1 Q_1)\cos\varphi - B_2 Q_2 \sin\varphi, \\ y' = (1 + B_1 Q_1)\sin\varphi + B_2 Q_2 \cos\varphi. \end{aligned} \tag{16}$$

The functions $\varphi,\ x,\ y$ are continuous at the point s_1.

To solve the formulated problem as one common BVP, we introduce the new nondimensional coordinate $0 \le \xi \le 1$:

$$\begin{aligned} &s \le s_1 :\ s = \xi s_1 \Rightarrow {}^{\mathrm{d}}\!/_{\mathrm{d}\xi} = s_1 {}^{\mathrm{d}}\!/_{\mathrm{d}s}; \\ &s_1 \le s \le L :\ s = L - \xi(L - s_1) \Rightarrow {}^{\mathrm{d}}\!/_{\mathrm{d}\xi} = -(L - s_1) {}^{\mathrm{d}}\!/_{\mathrm{d}s}. \end{aligned} \tag{17}$$

We combine the equations at both segments into a single system and distinguish the values by the indices $(\ldots)^{(1)},\ (\ldots)^{(2)}$. This transformation extents the formulation for the problem of laying process of an underwater pipeline [17] where the contact of an initially straight beam with a flat rigid surface is considered. A similar coordinate transformation can be found also in [22]. Thus, we obtain the BVP for the ninth-order ODE system:

$$Z' = G(\xi, Z), \quad Z \equiv \left(\sigma \quad \varphi^{(1)} \quad M^{(1)} \quad Q_1 \quad \varphi^{(2)} \quad x \quad y \quad M_* \quad s_1\right)^{\mathrm{T}}. \tag{18}$$

Here a prime indicates the derivative with respect to the new coordinate ξ (and the functions written in (18) are the functions of ξ). For the first four unknown variables, we have already derived Eq. (11). The remaining five equations are Eq. (16) and the conditions for the unknown constants: ${M_*}' = 0,\ {s_1}' = 0$.

Now we consider the boundary conditions for system (18) and note that the right end $\xi = 1$ corresponds to the unknown boundary of the contact segment $s = s_1$, whereas the left end corresponds to the start point $s = 0$ and the end point $s = L$. The conditions are:

$$\begin{aligned} &\xi = 0 :\ \ \sigma = 0,\ \varphi^{(1)} = \frac{\pi}{2},\ \varphi^{(2)} = 0; \\ &\xi = 1 :\ \ \varphi^{(1)} = \varphi^{(2)},\ Q_1 = \frac{P}{2}\cos\varphi,\ Q_2(\sigma, \varphi, Q_1) = -\frac{P}{2}\sin\varphi, \\ &\qquad M^{(1)} = \frac{P}{2}y + M_*,\ a_1(1 - \cos\kappa\sigma) = x,\ a_1 \sin\kappa\sigma = y. \end{aligned} \tag{19}$$

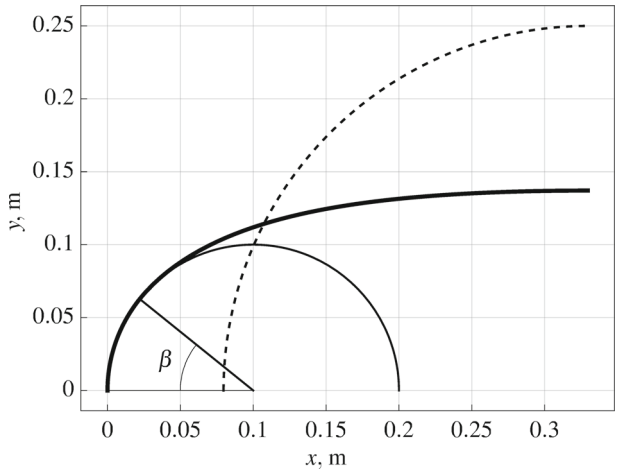

Fig. 3 Belt and pulley. The *thick line* is the deformed belt, the thin circle is the pulley, the *dashed line* is the undeformed belt, the thin line depicts the boundary of the contact segment

4 Numerical results

The formulated ninth-order BVP (18,19) is solved by the shooting method in MathCad using the standard built-in functions `sbval` and `rkfixed` [23]. The same results are also obtained using Wolfram Mathematica [9,34]. Here we apply two methods: the shooting method with the standard built-in function `NDSolve` and the finite difference method following the scheme described in [17].

In the finite difference method, we divide the segments into uniform steps $\varepsilon = 1/N$. To approximate the system, we use the implicit symmetric one-step difference scheme that has the second order of accuracy [3,29,32]: $(Y_{i+1} - Y_i)/\varepsilon = (G_i + G_{i+1})/2$, $(i = 0, \ldots, N-1)$. As a result of transformations, we obtain the system of $7N$ difference nonlinear algebraic equations. The total number of unknowns consists of the values of seven desired functions at the nodes $7(N+1)$ and two additional constants M_*, s_1. The system is complemented with nine boundary conditions (19) (in our case the Dirichlet boundary conditions) projected on the grid. It corresponds to the number of unknown variables: $7(N+1)$ values of variables at the nodes and two constants. The derived nonlinear algebraic system of equations is solved by Newton's method with the standard built-in function `FindRoot` of Wolfram Mathematica. We determine all the variable functions by interpolating the obtained values at the nodes (this also holds for the shooting method).

We suggest the use of the shooting method when an appropriate initial guess is not yet found, because we need only nine initial values here (while we need $7(N+1)+2$ values for the finite difference method). However, the finite difference method is faster and stabler; therefore, we advise it in any other cases.

The form of the belt before and after the deformation is shown in Fig. 3.

The parameters are: the Young modulus is $E = 10^9$ Pa, the Poisson coefficient is $\nu = 0.5$, the sides of the square cross section are $h = 10^{-2}$ m, the initial radius of the belt is $a_0 = 0.25$ m, the pulley radius is $a_1 = 0.1$ m, the current force is $P = 200$ N. $B_1 = 1/(Eh^2)$ is the tension compliance, $A = 12/(Eh^4)$ is the bending compliance, and $B_2 = 6/(5\mu h^2)$ is the shear compliance, where $\mu = E/(2(1+\nu))$. We calculate: the end coordinate of the contact segment $s_1 = 0.068$ m and the displacement of the pulley $\delta = 0.159$ m. The central angle of the contact zone is introduced in Fig. 3 and $\beta = 0.678$ in the example considered.

Next we determine the contact pressure using the formula (12). We take into account Eq. (8) and rewrite it as follows:

$$p = D^{-1}\left(Q_1{}' - \varphi' Q_2\right)\left[B_2 Q_2 + \frac{(1 + B_1 Q_1)^2}{B_2 Q_2}\right]. \tag{20}$$

The result of the calculation is shown in Fig. 4.

In Fig. 4, we see the concentration of pressure at the boundary of the contact segment which is characteristic for the problems with shear [17]. The pressure is positive, and its maximum equals 14.9×10^3 N/m. For considering the shear, there is no lumped boundary reaction force as in the model without shear [4,5]. For comparison, we draw the constant pressure from the equivalent (by the force P) problem without shear, but with tension, see the simpler modelling for this special case in [4]. Further on, we will mainly use these results

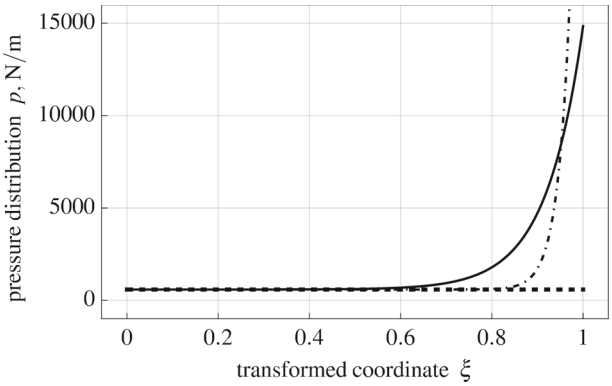

Fig. 4 Contact pressure over transformed coordinate. The *solid line* is the pressure for shearable model, the *dashed line* is the pressure in model without shear, and the *dot-dashed line* is the pressure in model with reduced shear compliance

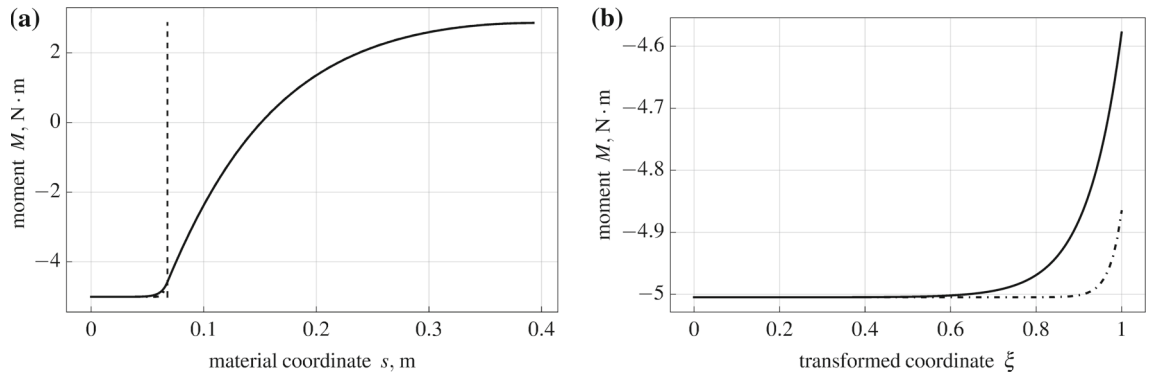

Fig. 5 Moment over material coordinate s in the whole belt (**a**) and moment over transformed coordinate (ξ) in the contact segment (**b**). The *dashed line* means the boundary between contact (*left side*) and free (*right side*) segments. The *dot-dashed line* is the model with reduced shear compliance

for comparison. In Fig. 4, we use $B_2^* = B_2/10$ for the model with the reduced shear compliance. We need to insert the new compliance into Eq. (20) and to obtain the new solution for the general system of Eqs. (18), (19). The reduction in the shear compliance results in sharpening of the pressure distribution, which in limiting case leads to constant pressure with the lumped force at the contact zone boundary.

The dependence of the moment in the belt on the material coordinate s is shown in Fig. 5. The moment is seen to vary in the contact segment. It takes place because Q_2 is not equal to zero in the shearable model [see Fig. 6 and (10)]. In contrast, the moment in the contact segment is constant if the unshearable model is considered.

For the problem without shear, cf. [4,5], the first component of force Q_1 is constant in the contact segment, and Q_2 is equal to zero. Besides in the case without shear, we have the lumped contact force at the contact segment boundary. As shown in Fig. 6, we have the qualitatively different results for these force components in the case with shear.

In Fig. 7, we draw the angle γ between the tangent vector $\mathbf{r}'$ and the unit vector $\mathbf{e}_1$. It increases at the contact segment up to the boundary point $s = s_1$ and decreases afterwards. The comparison with the results in [7] reveals qualitative similarities, and moreover, the magnitudes are of the same order. For the dashed line in Fig. 7, we use the reduced shear compliance $B_2^* = B_2/10$. The assumption "no shear at the beginning of the adhesive arc" in [21] and the similar one in [18] both give different results than those shown in Fig. 7 obtained for the frictionless contact.

Finally, we demonstrate a comparison between the loading diagrams of the models with shear and without it. To this end, we use the finite difference scheme (Wolfram Mathematica). The load P increases from zero, while other parameters are the same as above. We solve a number of static problems to show the dependences. The calculation results of previous steps are useful for the choice of appropriate initial approximations.

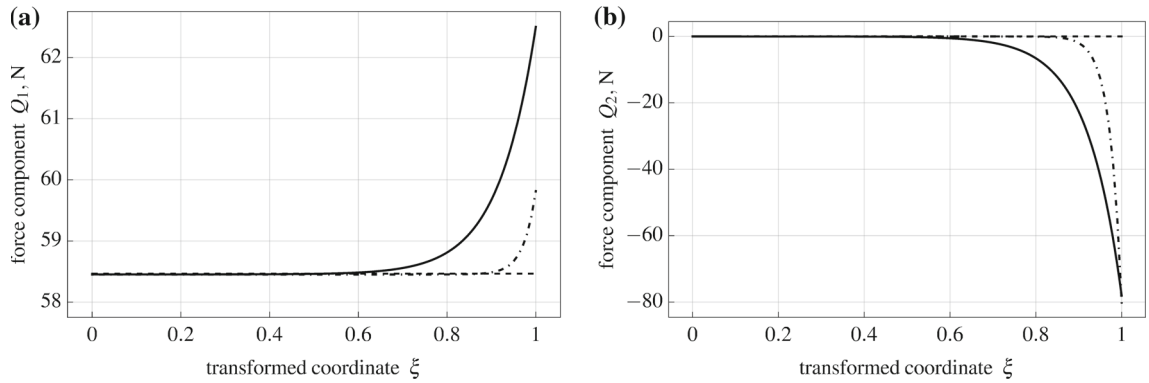

Fig. 6 Forces in the contact segment over transformed coordinate. First component (**a**) and second component (**b**). The *solid line* is the model with shear, the *dashed line* is the model without shear, and the *dot-dashed line* is the model with reduced shear compliance

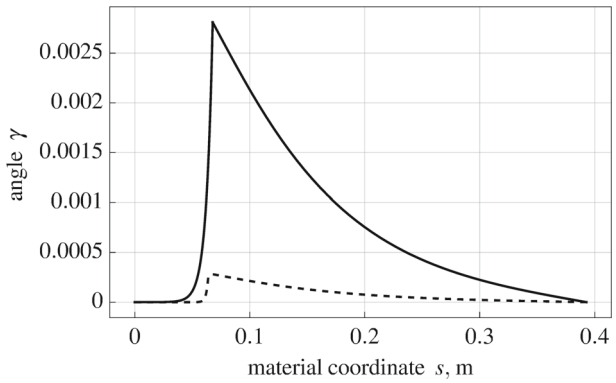

Fig. 7 Angle γ between tangent $\mathbf{r}'$ and unit vector $\mathbf{e}_1$ over material coordinate. The *dashed line* is the model with reduced shear compliance

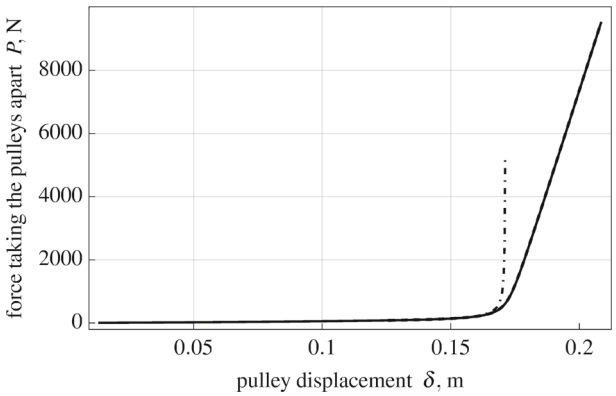

Fig. 8 Dependence of force on displacement of pulley. The *solid line* is the model with shear and extension, the *dashed line* is the model without shear (coinciding), and the *dot-dashed line* is the model without extension and shear

The dependence of the force $P(\delta)$ on the pulley displacement δ is depicted in Fig. 8. Any noticeable influence of shear is not observed here. For the model without extension and shear (dot-dashed line, see [5]), we see a limiting displacement for which the force tends to infinity.

The dependence $\beta(\delta)$ of the angle of the contact zone on the displacement of the pulley is shown in Fig. 9. The curve for the model with shear is smoother because of the absence of single force load at the contact area boundary. The contact zone becomes broader if the shear is included into consideration. The dot-dashed

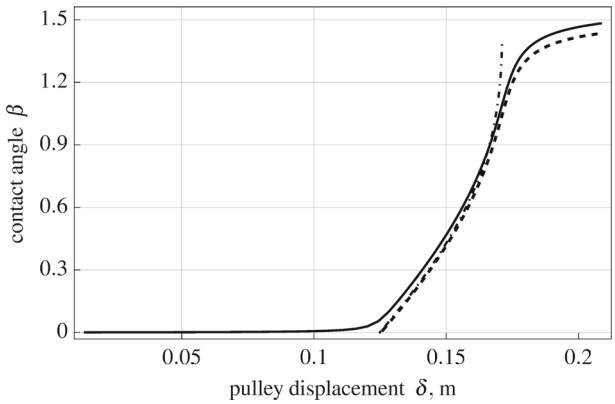

Fig. 9 Dependence of contact angle on displacement of pulley. The *solid line* is the model with shear and extension, the *dashed line* is the model without shear, and the *dot-dashed line* is the model without extension and shear

line shows the behaviour of the model without extension and shear, and it hardens when the displacement approaches the limiting value.

5 Conclusion

The main results of the present work are listed below:

- a system of ODE for the belt as plane nonlinear elastic rod with account for tension and transverse shear is derived;
- the equations for the free and contact segments which have qualitatively different formulation are combined into a single system of ODE. This system is suitable for numerical solving by the shooting method and finite difference method;
- computer mathematics is utilized for determining all the variables including the contact pressure;
- the important influence of shear in the belt–pulley problem is worked out clearly.

These results will be used in further work including the study of the belt–pulley interaction with friction and the dynamical modelling, both stationary and transient.

Acknowledgements Open access funding provided by Johannes Kepler University Linz. This research is carried out in the framework of the joint project of the Russian Foundation for Basic Research (Grant No. 14-51-15001) and the Austrian Science Fund (Grant No. I 2093 International Project).

References

1. Alciatore, D., Traver, A.: Multipulley belt drive mechanics: creep theory vs shear theory. ASME J. Mech. Des. **117**(4), 506–511 (1995). doi:10.1115/1.2826711
2. Antman, S.: Nonlinear Problems of Elasticity. Springer, New York (2005). doi:10.1007/0-387-27649-1
3. Bahvalov, N.S., Zhidkov, N.P., Kobelkov, G.G.: Numerical Methods. Binom. Laboratoria znanii, Moscow (2003)
4. Belyaev, A., Eliseev, V., Irschik, H., Oborin, E.: Nonlinear statics of extensible elastic belt on two pulleys. PAMM **16**(1), 11–14 (2016). doi:10.1002/pamm.201610004
5. Belyaev, A., Eliseev, V., Irschik, H., Oborin, E.: Contact of flexible elastic belt with two pulleys. In: Irschik, H., Belyaev, A., Krommer, M. (eds.) Dynamics & Control of Advanced Structures and Machines, pp. 195–203. Springer, Cham (2017). doi:10.1007/978-3-319-43080-5_22
6. Belyaev, A.K., Eliseev, V.V., Irschik, H., Oborin, E.: On static contact of belt and different pulleys. IOP Conf. Series Mater. Sci. Eng. **208**(1), 012004 (2017). doi:10.1088/1757-899X/208/1/012004
7. Belyaev, A.K., Eliseev, V.V., Oborin, E.A.: About one-dimensional models for describing elastic microslip in belt drive. Int. Rev. Mech. Eng. **10**(5), 333–338 (2016). doi:10.15866/ireme.v10i5.8944

8. Berger, E.: Friction modeling for dynamic system simulation. Appl. Mech. Rev. **55**(6), 535–577 (2002). doi:10.1115/1.1501080
9. Borwein, J., Skerritt, M.P.: An Introduction to Modern Mathematical Computing. Springer, New York (2012). doi:10.1007/978-1-4614-4253-0
10. Chen, J.S.: On the contact behavior of a buckled Timoshenko beam constrained laterally by a plane wall. Acta Mech. **222**(3), 225–232 (2011). doi:10.1007/s00707-011-0529-4
11. Dufva, K., Kerkkänen, K., Maqueda, L., Shabana, A.: Nonlinear dynamics of three-dimensional belt drives using the finite-element method. Nonlinear Dyn. **48**(4), 449–466 (2007). doi:10.1007/s11071-006-9098-9
12. Durville, D.: Contact-friction modeling within elastic beam assemblies: an application to knot tightening. Comput. Mech. **49**(6), 687–707 (2012). doi:10.1007/s00466-012-0683-0
13. Eliseev, V.: The non-linear dynamics of elastic rods. J. Appl. Math. Mech. **52**(4), 493–498 (1988)
14. Eliseev, V.: Saint-Venant problem and elastic moduli for bars with curvature and torsion. Izv. AN SSSR Mech. Solids **26**(2), 167–176 (1991)
15. Eliseev, V.: Mechanics of Deformable Solid Bodies. St.-Petersburg State Polytechnic University Publishing House, St. Petersburg (2006)
16. Eliseev, V., Vetyukov, Y.: Effects of deformation in the dynamics of belt drive. Acta Mech. **223**(8), 1657–1667 (2012). doi:10.1007/s00707-012-0675-3
17. Eliseev, V., Zinovieva, T.: Nonlinear-elastic strain of underwater pipeline in laying process. Comput. Contin. Mech. **5**(1), 70–78 (2012). doi:10.7242/1999-6691/2012.5.1.9
18. Firbank, T.: Mechanics of the belt drive. Int. J. Mech. Sci. **12**, 1053–1063 (1970)
19. Gasmi, A., Joseph, P.F., Rhyne, T.B., Cron, S.M.: Closed-form solution of a shear deformable, extensional ring in contact between two rigid surfaces. Int. J. Solids Struct. **48**(5), 843–853 (2011). doi:10.1016/j.ijsolstr.2010.11.018
20. Gasmi, A., Joseph, P.F., Rhyne, T.B., Cron, S.M.: The effect of transverse normal strain in contact of an orthotropic beam pressed against a circular surface. Int. J. Solids Struct. **49**, 2604–2616 (2012). doi:10.1016/j.ijsolstr.2012.05.022
21. Gerbert, G.: Traction Belt Mechanics. Chalmers University of Technology, Göteborg (1999)
22. Kaczmarczyk, S., Mirhadizadeh, S.: Quasi-stationary mechanics of elastic continua with bending stiffness wrapping on a pulley system. J. Phys. Conf. Ser. **721**(1), 012011 (2016). doi:10.1088/1742-6596/721/1/012011
23. Kiryanov, D., Kiryanova, E.: Computational Science. Infinity Science Press, Hingham (2007)
24. Kong, L., Parker, R.G.: Steady mechanics of belt-pulley systems. J. Appl. Mech. **72**(1), 25–34 (2005). doi:10.1115/1.1827251
25. Menq, C.H., Bielak, J., Griffin, J.: The influence of microslip on vibratory response. Part I: a new microslip model. J. Sound Vib. **107**(2), 279–293 (1986). doi:10.1016/0022-460X(86)90238-5
26. Morimoto, T., Iizuka, H.: Conformal contact between a rubber band and rigid cylinders. ASME J. Appl. Mech. **79**(4), 044504 (2012). doi:10.1115/1.4005566
27. Morimoto, T., Iizuka, H.: Rolling contact between a rubber ring and rigid cylinders: mechanics of rubber belts. Int. J. Mech. Sci. **54**(1), 234–240 (2012). doi:10.1016/j.ijmecsci.2011.11.001
28. Pechstein, A., Gerstmayr, J.: A Lagrange–Eulerian formulation of an axially moving beam based on the absolute nodal coordinate formulation. Multibody Syst. Dyn. **30**(3), 343–358 (2013). doi:10.1007/s11044-013-9350-2
29. Pozrikidis, C.: Numerical Computation in Science and Engineering. Oxford University Press, Oxford (2008)
30. Reynolds, O.: On the efficiency of belts or straps as communicators of work. Eng. **38**, 396 (1874)
31. Rubin, M.B.: An exact solution for steady motion of an extensible belt in multipulley belt drive systems. J. Mech. Des. **122**(3), 311–316 (2000). doi:10.1115/1.1288404
32. Samarskii, A.A., Vabishchevich, P.N.: Numerical Methods for Solving Inverse Problems of Mathematical Physics. No. 52 in Inverse and Ill-Posed Problems. De Gruyter, Berlin (2008)
33. Čepon, G., Boltežar, M.: Dynamics of a belt-drive system using a linear complementarity problem for the belt-pulley contact description. J. Sound Vib. **319**(3–5), 1019–1035 (2009). doi:10.1016/j.jsv.2008.07.005
34. Vetyukov, Y.: Nonlinear Mechanics of Thin-Walled Structures. Springer, Vienna (2014). doi:10.1007/978-3-7091-1777-40
35. Vetyukov, Y., Oborin, E., Krommer, M., Eliseev, V.: Transient modelling of flexible belt drive dynamics using the equations of a deformable string with discontinuities. Math. Comput. Model. Dyn. Syst. **23**(1), 40–54 (2017). doi:10.1080/13873954.2016.1232281
36. Villaggio, P.: Mathematical Models for Elastic Structures. Cambridge University Press, Cambridge (2005)
37. Wriggers, P., Laursen, T.A.: Computational Contact Mechanics. Springer, Berlin (2006). doi:10.1007/978-3-540-32609-0